Published in final edited form as:
J Comp Neurol. 2010 January 10; 518(2): 119–136. doi:10.1002/cne.22239.

Expression of PTPRO in the Interneurons of Adult Mouse Olfactory Bulb

Takenori Kotani[1], **Yoji Murata**[1], **Hiroshi Ohnishi**[1], **Munemasa Mori**[1], **Shinya Kusakari**[1], **Yasuyuki Saito**[1], **Hideki Okazawa**[1], **John L. Bixby**[2], and **Takashi Matozaki**[1,*]

[1]Laboratory of Biosignal Sciences, Institute for Molecular and Cellular Regulation, Gunma University, Maebashi, Gunma 371-8512, Japan

[2]Department of Molecular and Cellular Pharmacology, and Neuroscience Program, The Miami Project to Cure Paralysis, University of Miami Miller School of Medicine, Lois Pope LIFE Center, Miami, Florida 33136

Abstract

PTPRO is a receptor-type protein tyrosine phosphatase (PTP) with a single catalytic domain in its cytoplasmic region and multiple fibronectin type III-like domains in its extracellular region. In the chick, PTPRO mRNA has been shown to be particularly abundant in embryonic brain, and PTPRO is implicated in axon growth and guidance during embryonic development. However, the temporal and spatial expression of PTPRO protein in the mammalian CNS, particularly in the juvenile and adult mammalian brain, has not been evaluated in any detail. By immunohistofluorescence analysis with a monoclonal antibody to PTPRO, we show that PTPRO is widely expressed throughout the mouse brain from embryonic day 16 to postnatal day 1, while expression is largely confined to the olfactory bulb (OB) and olfactory tubercle in the adult brain. In the OB, PTPRO protein is expressed predominantly in the external plexiform layer, the granule cell layer, and the glomerular layer (GL). In these regions, expression of PTPRO is predominant in interneurons such as γ-aminobutyric acid (GABA)-ergic or calretinin (CR)-positive granule cells. In addition, PTPRO is expressed in GABAergic, CR-positive, tyrosine hydroxylase-positive, or neurocalcin-positive periglomerular cells in the GL. Costaining of PTPRO with other neuronal markers suggests that PTPRO is likely to be localized to the dendrites or dendritic spines of these olfactory interneurons. Thus, PTPRO might participate in regulation of dendritic morphology or synapse formation of interneurons in the adult mouse OB.

INDEXING TERMS

CNS; receptor-type tyrosine phosphatase; granule cells; periglomerular cells; localization; maturation

Protein tyrosine phosphatases (PTPs) play important roles in the development and function of the central nervous system (CNS; Paul and Lombroso, 2003). Based on amino acid sequence and cellular localization, PTPs have been classified into two groups: the receptor-type PTPs (RPTPs) and the nonreceptor type PTPs (Andersen et al., 2001; Alonso et al., 2004). RPTPs are further classified into eight subgroups (R1–R8 subtypes), largely according to the primary structures of their extracellular domains (Andersen et al., 2001). The majority of RPTPs except for CD45 (R1 subtype) are expressed in the CNS, and they

*CORRESPONDENCE TO: Takashi Matozaki, Laboratory of Biosignal Sciences, Institute for Molecular and Cellular Regulation, Gunma University, 3-39-15 Showa-Machi, Maebashi, Gunma 371-8512, Japan. matozaki@showa.gunma-u.ac.jp.

have been implicated in the regulation of neuronal adhesion and axon growth and guidance during CNS development (Paul and Lombroso, 2003; Lamprianou and Harroch, 2006).

Mammalian PTPRO (also known as GLEPP1, PTP-BK, or PTPφ) is an RPTP (R3 subtype; Andersen et al., 2001), with a single catalytic domain in its cytoplasmic region and seven or eight fibronectin type III-like domains in its extracellular region (Thomas et al., 1994; Tagawa et al., 1997; Tomemori et al., 2000). Indeed, five spliced isoforms of this PTP protein have been described (Beltran et al., 2003). Two transmembrane-type isoforms are highly expressed in the brain (Tagawa et al., 1997; Beltran et al., 2003) and podocytes of renal glomeruli (Wang et al., 1999; Wharram et al., 2000), and three truncated isoforms (PTPφ or PTPROt), which lack the extracellular domains, are expressed mainly in macrophages, B cells, or osteoclasts (Pixley et al., 1995; Wu et al., 1996; Aguiar et al., 1999). In the nervous system, PTPRO is implicated in axon growth and guidance during embryonic neurogenesis. In the chick brain, maximal expression of cPTPRO (previously named CRYP2), a chick homolog of mammalian PTPRO, was observed between embryonic day (E) 8 and E13, consistent with pervasive axon extension and tract formation in the chick CNS (Bodden and Bixby, 1996; Stepanek et al., 2001). The expression of cPTPRO is also concentrated at axons and growth cones of retinal projection neurons (Ledig et al., 1999). Depletion by RNAi of cPTPRO in developing motor neurons causes aberrant motor axon guidance (Stepanek et al., 2005). Biochemical analysis revealed that EphB receptor tyrosine kinase is a dephosphorylation substrate for cPTPRO (Shintani et al., 2006). Moreover, cPTPRO regulates the sensitivity of retinal axons to ephrins and hence has a crucial role in the establishment of retinotectal projection in the chick (Shintani et al., 2006).

By contrast, the localization and biological function of mammalian PTPRO in the CNS remain much less well investigated. The expression of PTPRO mRNA in the mouse brain was shown to peak from E16 to postnatal day (P) 3, and such expression was decreased afterward (Beltran et al., 2003), similar to the temporal expression pattern of cPTPRO mRNA. In situ hybridization showed that the expression of PTPRO transcripts is abundant in neocortical plate at E16 (Beltran et al., 2003). In contrast, the expression of PTPRO mRNA was prominent at the olfactory bulb (OB) at P2 (Beltran et al., 2003). In addition, moderate expression of PTPRO mRNA was observed in cerebral cortex and hippocampus, particularly in the granular layer of the dentate gyrus, at P2 (Beltran et al., 2003). However, the temporal and spatial expression of PTPRO protein in the mammalian CNS, particularly in the juvenile and adult mammalian brain, has not been evaluated in any detail. We have generated a monoclonal antibody (mAb) specific for mouse PTPRO and took advantage of this reagent to examine the detailed localization of this PTP in the developing and adult mouse brain.

MATERIALS AND METHODS

Animals

C57BL/6 mice of either sex were purchased from suppliers (Japan SLC, Inc., Hamamatsu, Japan; and CLEA Japan, Inc., Tokyo, Japan). For characterization of an mAb to mouse PTPRO, PTPRO-deficient mice (Wharram et al., 2000) were bred to homogeneity on a C57BL/6 × 129P3/J (*Ptpro*$^{-/-}$) background, and homozygous null mice and their wild-type littermates (at P1) were used. PTPRO-deficient mice were also back-crossed onto the C57BL/6 background for five generations, and homozygous null mice and their wild-type littermates (at 5 weeks of age) were used for the quantitative analysis of the synaptoporin-positive immunoreactivity in the OB. Animals were housed under a 12-hour light/dark cycle in standard animal cages and were provided with food and water ad libitum. All animals were maintained in the Institute of Experimental Animal Research of Gunma University

under specific pathogen-free conditions. All animal experiments were performed according to the guidelines of the Animal Care and Experimentation Committee of Gunma University.

Isolation of a full-length mouse PTPRO cDNA

A full-length mouse PTPRO cDNA (~3.7 kb) was isolated by reverse transcription-polymerase chain reaction (PCR) by the use of total RNA extracted from C57BL/6 mouse whole brain as described previously (Hayashi et al., 2004). The PCR primers were as follow: forward 5′-ggaattcgccatggggcacctgcctaggg-3′ and reverse 5′-gctcgtcgactaggacttgctgacgttctcg-3′. The resulting PCR product was subcloned into pBluescriptII (Stratagene, La Jolla, CA). The nucleotide sequences of the amplified cDNAs were verified by sequencing with ABI Prism 3100-Avant Genetic Analyzer (Applied Biosystems, Foster City, CA).

Plasmids

To construct an expression vector for mouse PTPRO, the full-length mouse PTPRO cDNA was subcloned into pcDNA3.1/myc-His (Invitrogen, Carlsbad, CA). To construct an expression vector for generation of a recombinant PTPRO-Fc fusion protein, in which the extracellular domain of mouse (amino acids 1–442) was fused with the Fc region of human immunoglobulin G (IgG), a DNA fragment corresponding to amino acids 1–442 of mouse PTPRO was amplified by PCR with the following primers: forward 5′-ggaattcgccatggggcacctgcctaggg-3′ and reverse 5′-ccgctctagacagttcttcaatccactcgcc-3′. The resulting PCR product was subcloned into pTracer-CMV-Fc vector as described previously (Hayashi et al., 2004). The nucleotide sequences of the amplified cDNAs were verified as described above. pEGFP-C2 vector for expression of enhanced green fluorescent protein (EGFP) was obtained from Clontech (Mountain View, CA).

Antibody characterization

See Table 1 for a list of all antibodies used.

Calbindin D28k (CB)—The rabbit polyclonal antibody (pAb) to CB recognized a single band of 28 kDa on immunoblot of rat hippocampal cells (Kim et al., 2006). This pAb does not react with calretinin and produces specific staining of Purkinje cells or their dendrites and axonal fibers in the cerebellum (technical information provided by Chemicon, Temecula, CA). The staining immunolabeling of human brain was abolished by the preadsorption of diluted antiserum (1:500) with 100 μM CB (Huynh et al., 2000). The staining pattern of CB in adult mouse OB in this study was identical to that in previous reports, in which the rabbit pAb to recombinant rat CB (Swant, Belinzona, Switzerland; CB-38) or the mouse mAb to bovine kidney CB (Sigma, St; Louis, MO; C-9848) was used (Parrish-Aungst et al., 2007; Batista-Brito et al., 2008).

Calretinin (CR)—The mouse mAb to CR recognized a single band of 31 kDa on immunoblot of ferret cochlear nucleus lysate (Fuentes-Santamaria et al., 2005). The staining of sections of adult mouse OB in this study produced a pattern of CR immunoreactivity that was identical to previous observations (Batista-Brito et al., 2008). It was also identical to the previous observations obtained with the use of the goat pAb to guinea pig CR (Millipore, Chemicon; AB1550; Parrish-Aungst et al., 2007).

EphA4—The rabbit pAb to EphA4 recognized a band of 120 kDa on immunoblot of the cell lysates of HEK293T cells exogenously expressing chick EphA4 (Shamah et al., 2001). The immunoreactivity with this pAb was reduced in the immunoblot of cell lysates from rat hippocampal neurons that were transfected with RNAi construct for EphA4 (Inoue et al.,

2009). This antibody was also useful for immunoprecipitation and immunoblot of mouse hippocampal neurons (data not shown).

GAD67—The mouse mAb to GAD67 recognized a single band of 67 kDa on immunoblot of rat cerebellar cortex (Fong et al., 2005). Immunohistochemistry of rat medulla showed a pattern similar to that reported previously from an in situ hybridization study (Fong et al., 2005). The staining of sections prepared from adult mouse OB in this study produced a pattern of GAD67 immunoreactivity that was identical to previous observations (Parrish-Aungst et al., 2007).

MAP2—The mouse mAb to MAP2 is immunospecific for all forms of MAP2, namely, MAP2a (280 kDa), MAP2b (280 kDa), and MAP2c (70 kDa), on immunoblot and does not react with other MAPs or tubulin (technical information provided by Sigma). This immunoreactivity was also absent in mice lacking MAP2 (Teng et al., 2001). Immunohistochemistory of brain tissue with this mAb shows selective labeling of dendrites throughout the brain (technical information provided by Sigma).

NeuN—The mouse mAb to NeuN recognized bands in the 46–48-kDa range in immunoblot of nuclear proteins from mouse brains (Mullen et al., 1992). This mAb reacts with most types of neuronal cells throughout the nervous system of mice, including cerebellum, cerebral cortex, hippocampus, thalamus, and spinal cord. The immunoreactivity of NeuN is detected in postmitotic neurons, but no staining with this mAb is observed in proliferative zones during the development of the brain (technical information provided by Millipore).

Neurocalcin (NC)—The rabbit pAb to NC recognizes a single band of 22 kDa on immunoblot of rat brain microsomal lysate (technical information provided by Enzo Life Science). This pAb produced the same staining pattern in the mouse OB as that of the rabbit pAb to bovine NC (De Marchis et al., 2007; Parrish-Aungst et al., 2007).

Parvalbumin (PV)—The mouse mAb to PV recognizes a band of 12 kDa on immunoblot and does not react with other members of the EF-hand family, such as calmodulin, S100A2 (S100L), S100A6 (calcyclin), myosin light chain, or troponin (technical information provided by Sigma). No staining with this mAb was observed in mice lacking PV (Burette et al., 2009).

Pgp9.5—The mouse mAb to Pgp9.5 recognized a single band of 27 kDa on immunoblot of the zebrafish and the rat brain (Trowern et al., 1996). The staining of sections from the mouse adult OB produced a pattern of Pgp9.5 immunoreactivity that was identical to the previous report (Imamura et al., 2006).

PTPRO—The information for the rat mAb to PTPRO is described below.

Synaptoporin—The rabbit pAb to synaptoporin recognized a single band of 37 kDa on immunoblot of the mouse hippocampus (Singec et al., 2002). The staining of sections from the mouse OB produced a pattern of synaptoporin immunoreactivity that was identical to a previous report (Whitman and Greer, 2007a).

Tyrosine hydroxylase (TH)—The mouse mAb to TH recognizes a band of approximately 59 – 61-kDa on immunoblot of the mouse brain and does not react with dopamine-β-hydroxylase, phenylalanine hydroxylase, tryptophan hydroxylase, dehydropteridine reductase, sepiapterin reductase, or phenethanolamine-N-methyl transferase on immunoblot (technical information provided by Millipore). The staining of

sections prepared from adult mouse OB produced a pattern of TH immunoreactivity that was identical to previous observations (Batista-Brito et al., 2008).

Generation of an mAb to mouse PTPRO

A rat mAb to mouse PTPRO (clone 591) was generated with the use of a recombinant PTPRO-Fc fusion protein as the antigen, as described previously (Hayashi et al., 2004; Sadakata et al., 2009). For the generation of mAbs, the purified PTPRO-Fc protein was injected into the hind foot pads of Wistar rats three times at 1-week intervals, after which lymphocytes were isolated from the draining lymph nodes and fused with P3U1 myeloma cells as described previously (Hayashi et al., 2004; Sadakata et al., 2009). Hybridoma clones producing mAbs that reacted with PTPRO-Fc but not with human IgG were identified by enzyme-linked immunosorbent assay. Among several positive clones, clone 591 was selected for experiments. The mAb was purified from serum-free culture supernatants of hybridoma cells by column chromatography on protein G-Sepharose 4FF (GE Healthcare, Buckinghamshire, United Kingdom).

Cell culture, transfection, and immunoblot analysis

HEK293 cells were maintained in Dulbecco's modified Eagle medium containing 10% fetal bovine serum at 37°C in 5% CO_2. They were transfected with pcDNA3.1/myc-His-PTPRO or pEGFP-C2 (as a negative control) with the use of LipofectAMINE2000 (Invitrogen) in accordance with manufacturer's procedure. For immunoblot analysis, the transfected cells were washed with ice-cold phosphate-buffered saline (PBS; pH 7.4) and then lysed with lysis buffer (20 mM Tris-HCl, pH 7.4, 150 mM NaCl, 2 mM ethylenediaminetetraacetic acid, 1% Nonidet P-40, 50 mM sodium fluoride, 1 mM phenylmethylsulfonyl fluoride, 10 μg/ml aprotinin, 1 mM sodium vanadate, 5 mM 2-mercaptoethanol). The lysates were centrifuged at 17,400*g* for 30 minutes at 4°C, and the resulting supernatants were subjected to immunoblot analysis as described by Murata et al. (2006). For immunoblot analysis of the brain, mice at P1 (*Ptpro*$^{+/+}$ and *Ptpro*$^{-/-}$) were sacrificed, and the whole brain was dissected into ice-cold PBS and homogenized in a Teflon homogenizer at 4°C in lysis buffer. The homogenates were rotated for 1 hour at 4°C and then centrifuged at 17,400*g* for 30 minutes at 4°C, with the resulting supernatants subjected to immunoblot analysis. Cell lysates prepared from transfected cells or mouse brain lysates were separated by 8% (see Fig. 1A) or 6% (see Fig. 1B) polyacrylamide gel, respectively and the separated proteins were transferred to nitrocellulose membranes. The membranes were blocked with a blocking solution [TBST (20 mM Tris-HCl, pH 7.6, 140 mM NaCl, 0.5% Tween 20) containing 1% bovine albumin serum] for 1 hour at room temperature and were then incubated with 0.4 μg/ml of the mAb to mouse PTPRO in blocking buffer at 4°C overnight. After washes with TBST, the membranes were incubated with horseradish peroxidase-conjugated goat pAbs to rat IgG (Jackson Immunoresearch, West Grove, PA) in blocking solution for 1 hour at room temperature, after which the membranes were washed with TBST. Immunoreactive bands were then detected with ECL Western blotting detection reagents (GE Healthcare) and LAS-3000 image analyzer (Fujifilm, Tokyo, Japan).

Immunohistofluorescence analysis

Mice at either E16 or P1 were anesthetized by brief chilling on ice. Mice at either P14 or 8 weeks after birth (P8w) were anesthetized by intraperitoneal injection of sodium pentobarbital at 25 mg/kg. After anesthetization, mice were perfused transcardially with saline containing 0.1% sodium nitrate and thereafter with 4% paraformaldehyde (PFA) in PBS. The brain was then dissected and postfixed with PBS containing 4% PFA for 6 hours at 4°C. Fixed tissues were transferred to 30% (w/v) sucrose in PBS for cryoprotection, embedded in OCT compound (Sakura Fine Technical, Tokyo, Japan), and rapidly frozen in

liquid nitrogen. Frozen sections with a thickness of 12 μm were prepared with a cryostat, mounted on glass slides, and air dried. All sections were then incubated for 1 hour at room temperature in buffer G (PBS containing 5% goat serum and 0.1% Triton X-100), after which they were incubated with primary antibodies (Table 1) diluted in buffer G overnight at 4°C. After washes in PBS, sections were incubated for 1 hour at room temperature with secondary antibodies conjugated with the fluorescent dye Cy3 or Alexa488. Cy3-labeled or Alexa488-labeled secondary antibodies were from Jackson Immunoresearch or from Invitrogen, respectively. Sections were then washed with PBS and treated with an antifading solution (20% polyvinyl alcohol, 5% 1,4-diazabicyclo[2.2.2]octane, 10% glycerol, 100 mM Tris-HCl, pH 9.0). For staining of nuclei, sections were incubated with 4′6-diamino-2-phenylindole (DAPI; 11034–56; 1:2,000) and secondary antibodies. DAPI was obtained from Nakarai Tesque (Kyoto, Japan). Fluorescence or confocal images were acquired with a fluorescence microscope BZ-8100 (Keyence, Osaka, Japan), a fluorescence microscope BX51 (Olympus, Tokyo, Japan), or a laser scanning confocal microscope LSM5 Pascal (Carl Zeiss, Oberkochen, Germany). Contrast and brightness of the photomicrographs were adjusted in Adobe Photoshop CS3 (Adobe Systems, San Jose, CA).

For determination of frequency and distribution of interneuron synapses in the OB, sagittal cryosections of the OB from wild-type and PTPRO-deficient mice at 5 weeks after birth were immunostained with pAbs to synaptoporin as described above. The stained sections were observed with an LSM5 Pascal, and confocal images were obtained. The number of synaptoporin-positive dots or the area occupied by synaptoporin immunoreactivity in the images was determined with ImageJ software (freely available at http://rsbweb.nih.gov/ij/).

RESULTS

Predominant expression of PTPRO protein in the OB of adult mice

To investigate the expression and localization of PTPRO protein, we generated an mAb to the extracellular region of mouse PTPRO. We first determined the specificity of this mAb by immunoblot analysis of cell lysates prepared from HEK293 cells transfected to express full-length mouse PTPRO cDNA (pcDNA3.1/myc-His-PTPRO). The immunoblot with this mAb to PTPRO revealed ~180–200-kDa immunoreactive bands in the cell lysates prepared from cells transfected with myc-His-tagged PTPRO cDNA but not in control-transfected cell lysates (Fig. 1A). The mAb also recognized ~170–200-kDa immunoreactive bands in the immunoblot of lysates prepared from the whole brain of wild-type mice at P1 (Fig. 1B). The molecular sizes of the immunoreactive bands correspond to those previously described (Wharram et al., 2000; Beltran et al., 2003). No reactive band was observed in the lysates prepared from the whole brain of PTPRO-deficient mice (Wharram et al., 2000; Fig. 1B). The immunoreactive bands of PTPRO in immunoblots appeared to be a doublet (Fig. 1A,B), which might be attributable to different modification of this protein by glycosylation.

Immunohistofluorescence staining with this mAb also revealed expression of PTPRO protein in the tectum of newborn mouse brain as well as in renal glomeruli; these signals were absent in sections from corresponding organs of PTPRO-deficient mice (Fig. 1C–F). Together, these results indicate that the mAb to PTPRO indeed recognizes endogenous mouse PTPRO.

We next examined the temporal and spatial expression patterns of PTPRO in the developing mouse brain by immunohistofluorescence analysis with our mAb to mouse PTPRO. Expression of PTPRO mRNA in the mouse brain is high from E16 to P3 and decreases in adulthood (Beltran et al., 2003). Consistent with these results, immunohistofluorescence analysis at either E16 or P1 revealed that the immunoreactivity of PTPRO was widely distributed throughout the brain and was particularly prominent in the OB, cerebral cortex,

basal forebrain, anterior commissure, hypothalamus, and midbrain (Fig. 2A,B). In contrast, by P14, the immunoreactivity of PTPRO was markedly decreased throughout the brain and was largely confined to the OB, the olfactory tubercle, and the dentate gyrus of hippocampus (Fig. 2C). At P8w, the immunoreactivity of PTPRO was localized almost exclusively to the OB and olfactory tubercle, whereas it was virtually undetectable in the rest of the brain (Fig. 2D).

Predominant expression of PTPRO in the γ-aminobutyric acid (GABA)ergic granule cells of the adult mouse OB

The OB is the first relay station in the olfactory system, in which odor information is transferred from the periphery to higher centers in the brain. It consists of various types of neurons and glia, forming five neuronal layer (Egger and Urban, 2006; Batista-Brito et al., 2008). The outermost layer in the OB is the olfactory nerve layer (ONL; see Fig. 3) composed by the axons projecting from the olfactory sensory neurons of the olfactory epithelium and olfactory ensheathing glia that enwrap these axons. The ONL is underlain by the glomerular layer (GL), where olfactory axons make synapses with primary dendrites of projection neurons and dendrites of interneurons. Projection neurons in the OB are tufted and mitral cells whose cell bodies are present in the third layer, the external plexiform layer (EPL), and the fourth layer, the mitral cell layer (MCL), respectively. The EPL also contains secondary dendrites of mitral and tufted cells that make dendrodendritic synapses with dendrites derived from granule cells. Granule cells in the OB are a major interneuron type that lacks axons (Egger and Urban, 2006). The cell bodies of most granule cells are located in the fifth layer, the granule cell layer (GCL). Granule cells also extend their dendrites into the EPL to form synapses with the mitral and tufted cells as described above. Predominant expression of PTPRO protein in the OB in adult mice thus prompted us to examine the detailed expression pattern of this PTP in the adult OB. Double staining with the mAb to mouse PTPRO and DAPI (for staining cell nuclei) showed that PTPRO protein was predominant in the EPL of the adult OB (Fig. 3). Moreover, strong PTPRO immunostaining was observed in the GL and GCL, whereas it was minimal in the MCL and ONL as well as at the border area between GL and EPL (Fig. 3).

To evaluate further the cell-type-specific expression of PTPRO in the adult OB, we performed double staining of the mouse OB at P8w for PTPRO and either MAP2 (Fig. 4A–F) or NeuN (Fig. 4G–I). PTPRO staining overlapped extensively with that of MAP2, a dendrite marker, in the EPL and GL as well as the outer layer of the GCL (Fig. 4A–C). At higher magnification (Fig. 4D–F), the PTPRO immunostaining appeared as a reticular pattern or dot-like structure in the EPL. In contrast, PTPRO staining did not overlap with that of MAP2 on the thick neurites, which might correspond to the dendrites derived from mitral/tufted cells (Fig. 4D–F, arrowheads). Moreover, staining for NeuN, a marker for the nucleus of mature neurons (Mullen et al., 1992), did not overlap with that of PTPRO in the GCL (Fig. 4G–I). Double staining of PTPRO and Pgp9.5, a marker for mitral/tufted cells in the adult OB (Weiler and Benali, 2005), showed that the staining of the former did not overlap with that of the latter in the MCL or EPL (Fig. 4J–L), suggesting that PTPRO is not expressed in mitral/tufted cells in the adult mouse OB. Thus, given that granule cells in the GCL extend their dendrites into the EPL, PTPRO is likely to be expressed in granule cells, particularly in the dendrites or dendritic spines.

A major population of granule cells in the GCL consists of GABAergic interneurons (Egger and Urban, 2006; Parrish-Aungst et al., 2007). To examine whether PTPRO is indeed expressed in granule cells, we thus performed immunohistofluorescence analysis in the adult OB with an mAb to GAD67, a GABA-synthesizing enzyme (Esclapez et al., 1994). Staining of GAD67 was predominant in the EPL and GL as well as the outer part of the GCL (Fig. 5A). GAD67 staining overlapped extensively with that of PTPRO in the EPL, which

contains granule cell dendrites (Fig. 5B). This merged staining was frequently observed as dot-like structures when viewed at higher magnification (Fig. 5C, arrows). The somas of GAD67-positive neurons were present in the GCL (Fig. 5D, arrowheads). However, PTPRO staining was minimal in the somas of GAD67-positive neurons in the GCL, whereas it overlapped with the dot-like GAD67-positive structures (Fig. 5D, arrows). Thus, these results suggest that PTPRO is expressed in the GABAergic granule cells in the EPL and in the GCL of the adult mouse OB. Moreover, PTPRO might be localized to dendrites or spines rather than the somas of the GABAergic granule cells. In addition to GAD67-positive neurons, CR-positive interneurons are also located mainly in the GL and GCL (Parrish-Aungst et al., 2007; Batista-Brito et al., 2008). CR staining partially overlapped with that of PTPRO in the GL, EPL, and GCL (Fig. 5E, F). At higher magnification, the merged staining was frequently observed as dot-like structures in the EPL (Fig. 5G, arrows). CR staining in the GCL was seen to overlap partially with that of PTPRO in the neuronal somas (Fig. 5H, arrowheads) as well as in neuritelike structures (Fig. 5H, arrows). We also identified PV-positive neurons in the EPL, as described previously (Parrish-Aungst et al., 2007; Batista-Brito et al., 2008). However, staining of PV did not overlap appreciably with that of PTPRO in either somas or neurites in the EPL (Fig. 5I–K). Thus, our results suggest that PTPRO is expressed preferentially in the CR-positive interneurons in the GCL or EPL but not in the PV-positive interneurons in the EPL.

Predominant expression of PTPRO in the GABAergic periglomerular cells of the adult mouse OB

PTPRO staining was also observed in the GL of the adult mouse OB (Figs. 3D,F, 4B). Given that the GABAergic granule cells in the EPL and GCL express PTPRO, we next examined whether specific types of interneurons in the GL also express PTPRO. Five subtypes of interneurons are known to be located in the GL, namely, CR-positive, PV-positive, TH-positive, CB-positive, and NC-positive interneurons (De Marchis et al., 2007; Parrish-Aungst et al., 2007; Batista-Brito et al., 2008). CR, PV, CB, and NC are all calcium-binding proteins (Parrish-Aungst et al., 2007). In addition, a subpopulation of the interneurons in the GL is also GABAergic (Parrish-Aungst et al., 2007). Staining of the GL with the mAb to PTPRO showed a meshwork-like staining, which enwrapped each glomerulus (Fig. 6B). Such staining of PTPRO partially overlapped with that of MAP2 in the GL (Fig. 6A–C, arrows). However, PTPRO staining did not overlap with the thick MAP2-positive neurites, likely to be dendrites derived from mitral/tufted cells (Fig. 6A–C, arrowheads). Similarly, a meshwork-like staining of GAD67 was observed in the GL, and it partially overlapped with that of PTPRO (Fig. 5A,B). At higher magnification, overlapping staining of PTPRO and GAD67 appeared as dot-like or neurite-like structures in the GL (Fig. 6D, arrows). In contrast, the somas of GAD67-positive neurons showed minimal staining for PTPRO (Fig. 6D, arrowheads).

PTPRO staining partially overlapped that of CR in the GL (Fig. 5E,F). At higher magnification, overlapping staining of PTPRO and CR was observed at neurite-like structures in the GL (Fig. 6E, arrows), whereas PTPRO staining was minimal in the somas of CR-positive neurons (Fig. 6E, arrowheads). PV staining was also observed in the GL (Fig. 5I). However, staining of PTPRO barely overlapped with that of PV in the GL at higher magnification (Fig. 6F). The staining pattern of TH in the GL was quite similar to that of CR (Figs. 5E,F, 6G,H). At higher magnification, PTPRO and TH staining coincided along neurite-like or dot-like structures (Fig. 6I, arrows). TH-positive neurons possess large somas compared with other subtypes of GL interneurons (Kosaka et al., 1998; Parrish-Aungst et al., 2007). PTPRO staining was frequently observed in the somas of TH-positive neurons (Fig. 6I, arrowheads). In contrast, the staining of CB in the GL was not seen to overlap with that of PTPRO (Fig. 6J–L). NC-positive periglomerular cells are also located in

the GL (Fig. 6M). In the GL, PTPRO staining partially overlapped with that of NC (Fig. 6N). At higher magnification, overlapping staining of PTPRO and NC was observed at neurite-like structures in the GL (Fig. 6O, arrows), whereas PTPRO staining was minimal in the somas of NC-positive neurons (Fig. 6O, arrowheads). Taken together, these results suggest that PTPRO is expressed in various types of GL interneurons, such as GAD67-, CR-, TH-, and NC-positive periglomerular cells, predominantly at their dendrites or spines.

PTPRO staining at dot-like structures in the EPL and GL suggests that PTPRO is localized to the dendritic spines of interneurons. We thus performed immunohistofluorescence analysis of the GL and the EPL with pAbs to synaptoporin, a presynaptic marker of granule cells (Whitman and Greer, 2007b). Synaptoporin staining overlapped extensively with that of PTPRO in the EPL and GL (Fig. 7A,B). At higher magnification, PTPRO staining frequently overlapped with dot-like synaptoporin-positive structures (Fig. 7C,D).

To investigate further whether PTPRO participates in the formation or the maintenance of dendrodendritic synapses of interneurons, we examined the frequency and distribution of interneuron synapses in the EPL of the adult OB in wild-type and PTPRO-deficient mice by immunostaining with the pAb to synaptoporin. Immunostaining pattern of synaptoporin in the EPL of PTPRO-deficient mice was dot-like and similar to that of wild-type mice (Fig. 7E,F). In addition, the number of synaptoporin-positive dots was comparable to that of wild-type mice (Fig. 7G). The total area stained with the pAb to synaptoporin in the EPL was also comparable between wild-type and PTPRO-deficient mice (Fig. 7H).

Colocalization of PTPRO and EphA4

Recently, EphA4 and EphB2, receptors for ephrins, were shown to be substrates for cPTPRO in the chick (Shintani et al., 2006). cPTPRO dephosphorylates a phosphorylated tyrosine residue in their juxtamembrane region, which is required for their activation and thereby negatively regulates the Eph signaling pathway (Shintani et al., 2006). In the OB, mouse EphA4 mRNA is expressed in the GCL (Liebl et al., 2003), and rat EphB2 protein has been detected in granule cells and periglomerular cells (St. John and Key, 2001). To investigate whether PTPRO is potentially involved in the regulation of Eph signaling in adult mouse OB, we performed immunostaining of PTPRO and EphA4 in the OB. As shown in Figure 8A,B, the immunoreactivities of EphA4 overlapped extensively with those of PTPRO in the GCL, EPL, and GL. At higher magnification, PTPRO staining also overlapped with EphA4 staining in GL and EPL (Fig. 8C,D).

DISCUSSION

We have found that PTPRO is expressed predominantly in the OB of adult mouse brain. Although PTPRO is widely expressed throughout the brain from E16 to P1, it becomes localized to the OB and olfactory tubercle in the adult brain. This general pattern of expression is consistent with, but expands upon, previous results from in situ hybridization (Beltran et al., 2003). In the present study, we investigated the detailed localization of PTPRO protein in the adult OB and showed that PTPRO is expressed predominantly in the EPL, GL, and GCL. Moreover, we show that PTPRO is expressed specifically in interneurons in the OB, such as granule cells and periglomerular cells. The interneurons in the OB consist of several subtypes of interneurons that are characterized by their location in the OB and expression of a variety of neuron markers, including GAD67, CR, PV, CB, TH, and NC (Parrish-Aungst et al., 2007). However, the functional differences among the subtypes of the interneurons in the OB have not been fully evaluated. In particular, PTPRO is expressed in GABAergic and CR-positive granule cells and in GABAergic, CR-positive, TH-positive, and NC-positive periglomerular cells. Interestingly, the staining of PTPRO in the EPL or GL is frequently colocalized with dot-like or neurite-like structures stained with

an Ab to MAP2, GAD67, CR, TH, or NC. In contrast, PTPRO staining was minimal in the somas of granule cells or periglomerular cells. Given that the staining of PTPRO is the most predominant in the EPL, where granule cell dendrites form dendrodendritic synapses with mitral and tufted cells, it is likely that PTPRO is localized specifically at the dendrites and/or spines of the granule cells or periglomerular cells. The colocalization of PTPRO with synaptoporin, a presynaptic marker in granule cells (Whitman and Greer, 2007b), in the EPL and the GL supports the idea that PTPRO is localized to synapses in these layers.

The functional role of PTPRO in OB interneurons remains unknown. OB interneurons are thought to be generated continuously from progenitor cells located in the subventricular zone (SVZ) of the cerebral cortex, which migrate toward the OB via the rostral migratory stream (RMS; Lledo and Saghatelyan, 2005; Duan et al., 2008). PTPRO was not detectable in the SVZ or RMS of 8-week-old mice (Kotani, Murata, Matozaki, unpublished data), so it is likely to be important for mature OB interneurons but not for proliferation or migration of newly generated interneurons. The expression of PTPRO is also predominant in the dentate gyrus at P14, although it declined in the adult mice (at P8w). Granule cells in the granule cell layer of the adult dentate gyrus are continuously and newly generated from neural stem cells in the subgranular zone (Duan et al., 2008), so PTPRO might also be important for granule cells in the dentate gyrus. Previous studies have shown that generation of the CB-positive periglomerular interneurons from progenitor cells predominates over that of TH- or CR-positive interneurons in newborn mice, whereas generation of the latter cell types predominates during adulthood (De Marchis et al., 2007). Moreover, bromodeoxyuridine (BrdU) incorporation was markedly greater in GABAergic, TH-positive, or CR-positive periglomerular interneurons in the adult compared with that in CB- or PV-positive periglomerular interneurons (Whitman and Greer, 2007a). We showed that expression of PTPRO was high in GABAergic, TH-positive, or CR-positive interneurons but minimal in the CB- or PV-positive cells. Indeed, triple-labeling studies with Abs to PTPRO, BrdU, and interneuron markers (GAD67, CR, CB, or PV) showed that BrdU-positive neurons tended to be PTPRO/GAD67 or PTPRO/CR double positive but not CB or PV positive (Kotani, Murata, Matozaki, unpublished data). Taken together, these data suggest that PTPRO is preferentially expressed in the subpopulation of olfactory interneurons that experiences accelerated turnover in the adult OB.

PTPRO is concentrated in the growth cones of retinal projection neurons in chick (Ledig et al., 1999) and in the apical surface of foot processes in the highly polarized glomerular epithelial cells (Yang et al., 1996; Wharram et al., 2000). Although the morphology of foot processes is distinct from that of neuronal dendrites or growth cones, each of these structures is rich in actin (Benzing, 2004; Dehmelt and Halpain, 2004; Faul et al., 2007; Penzes et al., 2008). Signaling by protein tyrosine phosphorylation/dephosphorylation in neurons is implicated in reorganization of the actin cytoskeleton through Rho-family small GTPases, resulting in growth of axons and dendrites as well as synapse formation (Negishi and Katoh, 2002; Govek et al., 2005). Thus, PTPRO might participate in development or remodeling of interneuron spines and dendrites, thereby regulating the plasticity of synapse formation between interneurons and primary and/or secondary olfactory neurons. Recently, receptors for ephrinB ligands, EphA4 and EphB2, were shown to be substrates for PTPRO (Shintani et al., 2006). Binding of ephrinBs leads to autophosphorylation of Eph receptors at several tyrosine residues, resulting in activation of downstream signaling cascades (Binns et al., 2000; Goldshmit et al., 2006). Thus, PTPRO is likely to be a negative regulator of ephrin-Eph signaling (Shintani et al., 2006). This is relevant to the present study because EphA4 mRNA is expressed in the GCL of the mouse OB (Liebl et al., 2003), and EphB2 protein has been detected in granule cells and periglomerular cells in the rat OB (St. John and Key, 2001). The present study also showed that the staining of PTPRO overlapped with that of EphA4 in the GL, EPL, and GCL of the adult mouse OB. Eph receptors are thought to

regulate the reorganization of the actin cytoskeleton through Rho-family small G proteins (Huot, 2004), and they are known to regulate synaptogenesis (Henkemeyer et al., 2003; Bouvier et al., 2008). Thus, PTPRO might participate in the regulation of synapse formation of OB interneurons through modulation of ephrin–Eph signaling.

In a histological study of the OB in the adult PTPRO-deficient mice, no differences were observed between wild-type and PTPRO-deficient animals with regard to hematoxylin-eosin staining or immunostaining for various OB markers as used in the present study (Kotani, Murata, Matozaki, unpublished data). In addition, by immunostaining of synaptoporin, no difference was observed in the frequency and distribution of dendrodendritic synapses in the adult OB among the genotypes, suggesting that PTPRO is unlikely to participate in the formation or the maintenance of these synapses. However, at least 18 different RPTPs are expressed in the brain. In particular, by searching the Allen Brain Atlas database (http://mouse.brain-map.org/welcome.do), we found that both RPTPσ and RPTPζ mRNAs are highly expressed in the adult OB. In addition, LAR RPTP mRNA is expressed in the adult OB (Schaapveld et al., 1998). These data suggest that these RPTPs might be able to compensate for the loss of PTPRO. Moreover, the present study strongly suggests a potential role of PTPRO in regulation of the olfactory activity. Thus, further examination including behavioral tests for the olfaction will be necessary to investigate the physiological function of PTPRO in the adult mouse brain.

Acknowledgments

We thank Dr. R.C. Wiggins (University of Michigan) for his permission to obtain and use PTPRO-deficient mice and Manuel Gonzalez-Brito for breeding these mice onto a homogeneous background. We also thank Y. Kusakari, E. Urano, and H. Kobayashi for technical assistance.

Grant sponsor: The Ministry of Education, Culture, Sports, Science, and Technology of Japan; Grant number: 20370044 (to T.M.), Grant number: 1979025 (to Y.M.); Grant sponsor: National Institutes of Health; Grant number: NS38920 (to J.L.B.).

Abbreviations

AC	anterior commissure
BF	basal forebrain
Ctx	cerebral cortex
EPL	external plexiform layer
GCL	granule cell layer
GL	glomerular layer
Hip	hippocampus
Hth	hypothalamus
MCL	mitral cell layer
Mid	midbrain
NeuN	neuronal nuclei
OB	olfactory bulb
ONL	olfactory nerve layer
RMS	rostral migratory stream
SVZ	subventricular zone

Te	tectum
Tu	olfactory tubercle

LITERATURE CITED

Aguiar RC, Yakushijin Y, Kharbanda S, Tiwari S, Freeman GJ, Shipp MA. PTPROt: an alternatively spliced and developmentally regulated B-lymphoid phosphatase that promotes G0/G1 arrest. Blood. 1999; 94:2403–2413. [PubMed: 10498613]

Alonso A, Sasin J, Bottini N, Friedberg I, Friedberg I, Osterman A, Godzik A, Hunter T, Dixon J, Mustelin T. Protein tyrosine phosphatases in the human genome. Cell. 2004; 117:699–711. [PubMed: 15186772]

Andersen JN, Mortensen OH, Peters GH, Drake PG, Iversen LF, Olsen OH, Jansen PG, Andersen HS, Tonks NK, Møller NP. Structural and evolutionary relationships among protein tyrosine phosphatase domains. Mol Cell Biol. 2001; 21:7117–7136. [PubMed: 11585896]

Batista-Brito R, Close J, Machold R, Fishell G. The distinct temporal origins of olfactory bulb interneuron subtypes. J Neurosci. 2008; 28:3966–3975. [PubMed: 18400896]

Beltran PJ, Bixby JL, Masters BA. Expression of PTPRO during mouse development suggests involvement in axonogenesis and differentiation of NT-3- and NGF-dependent neurons. J Comp Neurol. 2003; 456:384–395. [PubMed: 12532410]

Benzing T. Signaling at the slit diaphragm. J Am Soc Nephrol. 2004; 15:1382–1391. [PubMed: 15153549]

Binns KL, Taylor PP, Sicheri F, Pawson T, Holland SJ. Phosphorylation of tyrosine residues in the kinase domain and juxtamembrane region regulates the biological and catalytic activities of Eph receptors. Mol Cell Biol. 2000; 20:4791–4805. [PubMed: 10848605]

Bodden K, Bixby JL. CRYP-2: a receptor-type tyrosine phosphatase selectively expressed by developing vertebrate neurons. J Neurobiol. 1996; 31:309–324. [PubMed: 8910789]

Bouvier D, Corera AT, Tremblay ME, Riad M, Chagnon M, Murai KK, Pasquale EB, Fon EA, Doucet G. Pre-synaptic and post-synaptic localization of EphA4 and EphB2 in adult mouse forebrain. J Neurochem. 2008; 106:682–695. [PubMed: 18410519]

Burette AC, Strehler EE, Weinberg RJ. “Fast” plasma membrane calcium pump PMCA2a concentrates in GABAergic terminals in the adult rat brain. J Comp Neurol. 2009; 512:500–513. [PubMed: 19025983]

De Marchis S, Bovetti S, Carletti B, Hsieh YC, Garzotto D, Peretto P, Fasolo A, Puche AC, Rossi F. Generation of distinct types of periglomerular olfactory bulb interneurons during development and in adult mice: implication for intrinsic properties of the subventricular zone progenitor population. J Neurosci. 2007; 27:657–664. [PubMed: 17234597]

Dehmelt L, Halpain S. Actin and microtubules in neurite initiation: are MAPs the missing link? J Neurobiol. 2004; 58:18–33. [PubMed: 14598367]

Duan X, Kang E, Liu CY, Ming GL, Song H. Development of neural stem cell in the adult brain. Curr Opin Neurobiol. 2008; 18:108–115. [PubMed: 18514504]

Egger V, Urban NN. Dynamic connectivity in the mitral cell– granule cell microcircuit. Semin Cell Dev Biol. 2006; 17:424–432. [PubMed: 16889994]

Esclapez M, Tillakaratne NJ, Kaufman DL, Tobin AJ, Houser CR. Comparative localization of two forms of glutamic acid decarboxylase and their mRNAs in rat brain supports the concept of functional differences between the forms. J Neurosci. 1994; 14:1834–1855. [PubMed: 8126575]

Faul C, Asanuma K, Yanagida-Asanuma E, Kim K, Mundel P. Actin up: regulation of podocyte structure and function by components of the actin cytoskeleton. Trends Cell Biol. 2007; 17:428–437. [PubMed: 17804239]

Fong AY, Stornetta RL, Foley CM, Potts JT. Immunohistochemical localization of GAD67-expressing neurons and processes in the rat brainstem: subregional distribution in the nucleus tractus solitarius. J Comp Neurol. 2005; 493:274–290. [PubMed: 16255028]

Fuentes-Santamaria V, Alvarado JC, Taylor AR, Brunso-Bechtold JK, Henkel CK. Quantitative changes in calretinin immunostaining in the cochlear nuclei after unilateral cochlear removal in young ferrets. J Comp Neurol. 2005; 483:458–475. [PubMed: 15700274]

Goldshmit Y, McLenachan S, Turnley A. Roles of Eph receptors and ephrins in the normal and damaged adult CNS. Brain Res Rev. 2006; 52:327–345. [PubMed: 16774788]

Govek EE, Newey SE, Van Aelst L. The role of the Rho GTPases in neuronal development. Genes Dev. 2005; 19:1–49. [PubMed: 15630019]

Hayashi A, Ohnishi H, Okazawa H, Nakazawa S, Ikeda H, Motegi S, Aoki N, Kimura S, Mikuni M, Matozaki T. Positive regulation of phagocytosis by SIRPβ and its signaling mechanism in macrophages. J Biol Chem. 2004; 279:29450–29460. [PubMed: 15123631]

Henkemeyer M, Itkis OS, Ngo M, Hickmott PW, Ethell IM. Multiple EphB receptor tyrosine kinases shape dendritic spines in the hippocampus. J Cell Biol. 2003; 163:1313–1326. [PubMed: 14691139]

Huot J. Ephrin signaling in axon guidance. Prog Neuropsychopharmacol Biol Psychiatry. 2004; 28:813–818. [PubMed: 15363605]

Huynh DP, Figueroa K, Hoang N, Pulst SM. Nuclear localization or inclusion body formation of ataxin-2 are not necessary for SCA2 pathogenesis in mouse or human. Nat Genet. 2000; 26:44–50. [PubMed: 10973246]

Imamura F, Nagao H, Naritsuka H, Murata Y, Taniguchi H, Mori K. A leucine-rich repeat membrane protein, 5T4, is expressed by a subtype of granule cells with dendritic arbors in specific strata of the mouse olfactory bulb. J Comp Neurol. 2006; 495:754–768. [PubMed: 16506198]

Inoue E, Deguchi-Tawarada M, Togawa A, Matsui C, Arita K, Katahira-Tayama S, Sato T, Yamauchi E, Oda Y, Takai Y. Synaptic activity prompts γ-secretase-mediated cleavage of EphA4 and dendritic spine formation. J Cell Biol. 2009; 185:551–564. [PubMed: 19414612]

Kim JH, Lee JA, Song YM, Park CH, Hwang SJ, Kim YS, Kaang BK, Son H. Overexpression of calbindin-D28K in hippocampal progenitor cells increases neuronal differentiation and neurite outgrowth. FASEB J. 2006; 20:109–111. [PubMed: 16278289]

Kosaka K, Toida K, Aika Y, Kosaka T. How simple is the organization of the olfactory glomerulus? The heterogeneity of so-called periglomerular cells. Neurosci Res. 1998; 30:101–110. [PubMed: 9579643]

Lamprianou S, Harroch S. Receptor protein tyrosine phosphatase from stem cells to mature glial cells of the central nervous system. J Mol Neurosci. 2006; 29:241–255. [PubMed: 17085782]

Ledig MM, McKinnell IW, Mrsic-Flogel T, Wang J, Alvares C, Mason I, Bixby JL, Mueller BK, Stoker AW. Expression of receptor tyrosine phosphatases during development of the retinotectal projection of the chick. J Neurobiol. 1999; 39:81–96. [PubMed: 10213455]

Liebl DJ, Morris CJ, Henkemeyer M, Parada LF. mRNA expression of ephrins and Eph receptor tyrosine kinases in the neonatal and adult mouse central nervous system. J Neurosci Res. 2003; 71:7–22. [PubMed: 12478610]

Lledo PM, Saghatelyan A. Integrating new neurons into the adult olfactory bulb: joining the network, life-death decisions, and the effects of sensory experience. Trends Neurosci. 2005; 28:248–254. [PubMed: 15866199]

Mullen RJ, Buck CR, Smith AM. NeuN, a neuronal specific nuclear protein in vertebrates. Development. 1992; 116:201–211. [PubMed: 1483388]

Murata T, Ohnishi H, Okazawa H, Murata Y, Kusakari S, Hayashi Y, Miyashita M, Itoh H, Oldenborg PA, Furuya N, Matozaki T. CD47 promotes neuronal development through Srcand FRG/Vav2-mediated activation of Rac and Cdc42. J Neurosci. 2006; 26:12397–12407. [PubMed: 17135401]

Negishi M, Katoh H. Rho family GTPases as key regulators for neuronal network formation. J Biochem. 2002; 132:157–166. [PubMed: 12153710]

Parrish-Aungst S, Shipley MT, Erdelyi F, Szabo G, Puche AC. Quantitative analysis of neuronal diversity in the mouse olfactory bulb. J Comp Neurol. 2007; 501:825–836. [PubMed: 17311323]

Paul S, Lombroso PJ. Receptor and nonreceptor protein tyrosine phosphatases in the nervous system. Cell Mol Life Sci. 2003; 60:2465–2482. [PubMed: 14625689]

Penzes P, Cahill ME, Jones KA, Srivastava DP. Convergent CaMK and RacGEF signals control dendritic structure and function. Trends Cell Biol. 2008; 18:405–413. [PubMed: 18701290]

Pixley FJ, Lee PS, Dominguez MG, Einstein DB, Stanley ER. A heteromorphic protein-tyrosine phosphatase, PTPφ, is regulated by CSF-1 in macrophages. J Biol Chem. 1995; 270:27339–27347. [PubMed: 7592997]

Sadakata H, Okazawa H, Sato T, Supriatna Y, Ohnishi H, Kusakari S, Murata Y, Ito T, Nishiyama U, Minegishi T, Harada A, Matozaki T. SAP-1 is a microvillus-specific protein tyrosine phosphatase that modulates intestinal tumorigenesis. Genes Cells. 2009; 14:295–308. [PubMed: 19170756]

Schaapveld RQ, Schepens JT, Bächner D, Attema J, Wieringa B, Jap PH, Hendriks WJ. Developmental expression of the cell adhesion molecule-like protein tyrosine phosphatases LAR, RPTPδ and RPTPα in the mouse. Mech Dev. 1998; 77:59–62. [PubMed: 9784606]

Shamah SM, Lin MZ, Goldberg JL, Estrach S, Sahin M, Hu L, Bazalakova M, Neve RL, Corfas G, Debant A, Greenberg ME. EphA receptors regulate growth cone dynamics through the novel guanine nucleotide exchange factor ephexin. Cell. 2001; 105:233–244. [PubMed: 11336673]

Shintani T, Ihara M, Sakuta H, Takahashi H, Watakabe I, Noda M. Eph receptors are negatively controlled by protein tyrosine phosphatase receptor type O. Nat Neurosci. 2006; 9:761–769. [PubMed: 16680165]

Singec I, Knoth R, Ditter M, Hagemeyer CE, Rosenbrock H, Frotscher M, Volk B. Synaptic vesicle protein synaptoporin is differently expressed by subpopulations of mouse hippocampal neurons. J Comp Neurol. 2002; 452:139–153. [PubMed: 12271488]

St. John JA, Key B. EphB2 and two of its ligands have dynamic protein expression patterns in the developing olfactory system. Brain Res Dev Brain Res. 2001; 126:43–56.

Stepanek L, Sun QL, Wang J, Wang C, Bixby JL. CRYP-2/cPTPRO is a neurite inhibitory repulsive guidance cue for retinal neurons in vitro. J Cell Biol. 2001; 154:867–878. [PubMed: 11514594]

Stepanek L, Stoker AW, Stoeckli E, Bixby JL. Receptor tyrosine phosphatases guide vertebrate motor axons during development. J Neurosci. 2005; 25:3813–3823. [PubMed: 15829633]

Tagawa M, Shirasawa T, Yahagi Y, Tomoda T, Kuroyanagi H, Fujimura S, Sakiyama S, Maruyama N. Identification of a receptor-type protein tyrosine phosphatase expressed in postmitotic maturing neurons: its structure and expression in the central nervous system. Biochem J. 1997; 321:865–871. [PubMed: 9032477]

Teng J, Takei Y, Harada A, Nakata T, Chen J, Hirokawa N. Synergistic effects of MAP2 and MAP1B knockout in neuronal migration, dendritic outgrowth, and microtubule organization. J Cell Biol. 2001; 155:65–76. [PubMed: 11581286]

Thomas PE, Wharram BL, Goyal M, Wiggins JE, Holzman LB, Wiggins RC. GLEPP1, a renal glomerular epithelial cell (podocyte) membrane protein-tyrosine phosphatase. Identification, molecular cloning, and characterization in rabbit. J Biol Chem. 1994; 269:19953–19962. [PubMed: 7519601]

Tomemori T, Seki N, Suzuki Y, Shimizu T, Nagata H, Konno A, Shirasawa T. Isolation and characterization of murine orthologue of PTP-BK. Biochem Biophys Res Commun. 2000; 276:974–981. [PubMed: 11027578]

Trowern AR, Laight R, MacLean N, Mann DA. Detection of neuron-specific protein gene product (PGP) 9.5 in the rat and zebrafish using anti-human PGP9.5 antibodies. Neurosci Lett. 1996; 210:21–24. [PubMed: 8762182]

Wang R, St John PL, Wiggins RC, Abrahamson DR. 32 molecular cloning and expression of glomerular epithelial protein 1 (GLEPP1) in developing mouse kidney. J Histochem Cytochem. 1999; 47:1650. [PubMed: 10567479]

Weiler E, Benali A. Olfactory epithelia differentially express neuronal markers. J Neurocytol. 2005; 34:217–240. [PubMed: 16841165]

Wharram BL, Goyal M, Gillespie PJ, Wiggins JE, Kershaw DB, Holzman LB, Dysko RC, Saunders TL, Samuelson LC, Wiggins RC. Altered podocyte structure in GLEPP1 (Ptpro)- deficient mice associated with hypertension and low glomerular filtration rate. J Clin Invest. 2000; 106:1281–1290. [PubMed: 11086029]

Whitman MC, Greer CA. Adult-generated neurons exhibit diverse developmental fates. Dev Neurobiol. 2007a; 67:1079–1093. [PubMed: 17565001]

Whitman MC, Greer CA. Synaptic integration of adult-generated olfactory bulb granule cells: basal axodendritic centrifugal input precedes apical dendrodendritic local circuits. J Neurosci. 2007b; 27:9951–9961. [PubMed: 17855609]

Wu LW, Baylink DJ, Lau KH. Molecular cloning and expression of a unique rabbit osteoclastic phosphotyrosyl phosphatase. Biochem J. 1996; 316:515–523. [PubMed: 8687395]

Yang DH, Goyal M, Sharif K, Kershaw D, Thomas P, Dysko R, Wiggins R. Glomerular epithelial protein 1 and podocalyxin-like protein 1 in inflammatory glomerular disease (crescentic nephritis) in rabbit and man. Lab Invest. 1996; 74:571–584. [PubMed: 8600307]

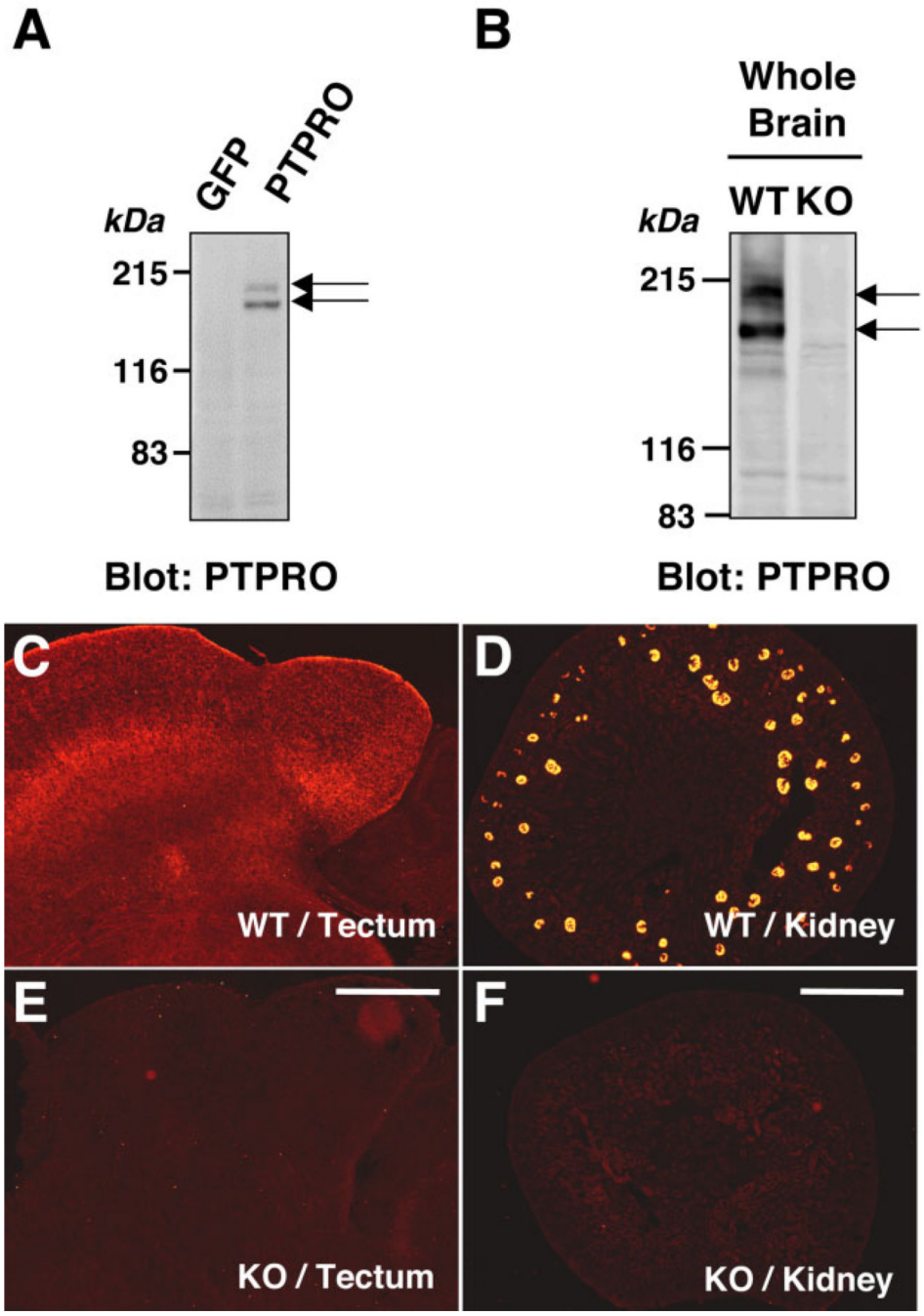

Figure 1.

Specificity of a mAb to mouse PTPRO. **A:** Cell lysates from HEK293 cells transfected with an expression vector containing enhanced green fluorescent protein cDNA (GFP; as a negative control) or myc-His tagged PTPRO cDNA (PTPRO) subjected to immunoblot analysis with the mAb (clone 591) to mouse PTPRO. The ~180–200-kDa immunoreactive bands (arrows) are observed in the cell lysates from cells transfected with PTPRO cDNA but not in the control lysates. **B:** Lysates (20 μg of protein) prepared from the whole brain of either wild-type (WT) or PTPRO-deficient (KO) mice subjected to immunoblot analysis with the mAb to PTPRO. The ~170–200-kDa immunoreactive bands (arrows) are detected

in the lysates from WT mice but not those from PTPRO-deficient mice. The positions of molecular size standards are indicated at left (A,B). **C–F:** Cryosections of the mouse brain (C,E, the tectum area) and kidney (D,F) from either WT (C,D) or PTPRO-deficient (E,F) mice at P1 immunostained with the mAb to PTPRO. Strong PTPRO immunoreactivity is observed in the tectum and renal glomeruli of the WT mouse but not of the PTPRO-deficient mouse. The images for C–F were acquired with a fluorescence microscope (BX51, Olympus). Scale bars = 500 μm in E (applies to C,E); 500 μm in F (applies to D,F).

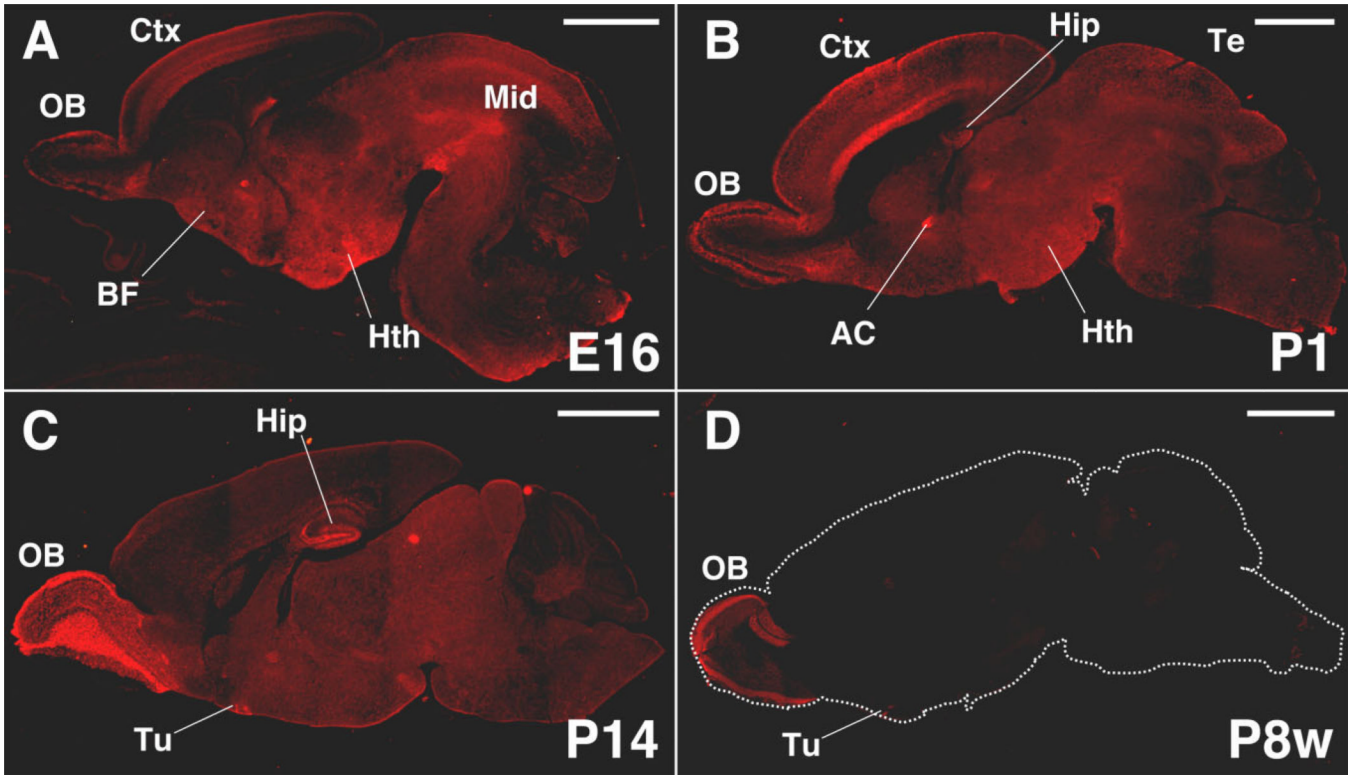

Figure 2.

Distribution of PTPRO immunoreactivity in sagittal sections of the developing and mature mouse brain. Sagittal cryosections of the brain from the mice at embryonic day (E) 16 to 8 weeks after birth (P8w) were immunostained with the mAb to PTPRO. **A:** At E16, PTPRO immunoreactivity is widely distributed throughout the brain and is particularly prominent in the olfactory bulb (OB), cerebral cortex (Ctx), basal forebrain (BF), hypothalamus (Hth), and midbrain (Mid). **B:** At postnatal day (P) 1, PTPRO immunoreactivity is widely distributed throughout the brain, with high levels in the OB, Ctx (especially in the motor cortex), anterior commissure (AC), Hth, hippocampus (Hip), and tectum (Te). **C:** At P14, PTPRO immunoreactivity in the brain is markedly decreased compared with earlier stages and is localized to the OB, olfactory tubercle (Tu), and dentate gyrus of hippocampus. **D:** At P8w, PTPRO immunoreactivity is localized to the OB and Tu and is virtually undetectable in the rest of the brain. All images were acquired with a fluorescence microscope (BZ-8100; Keyence). Scale bars = 1 mm in A,B; 2 mm in C,D.

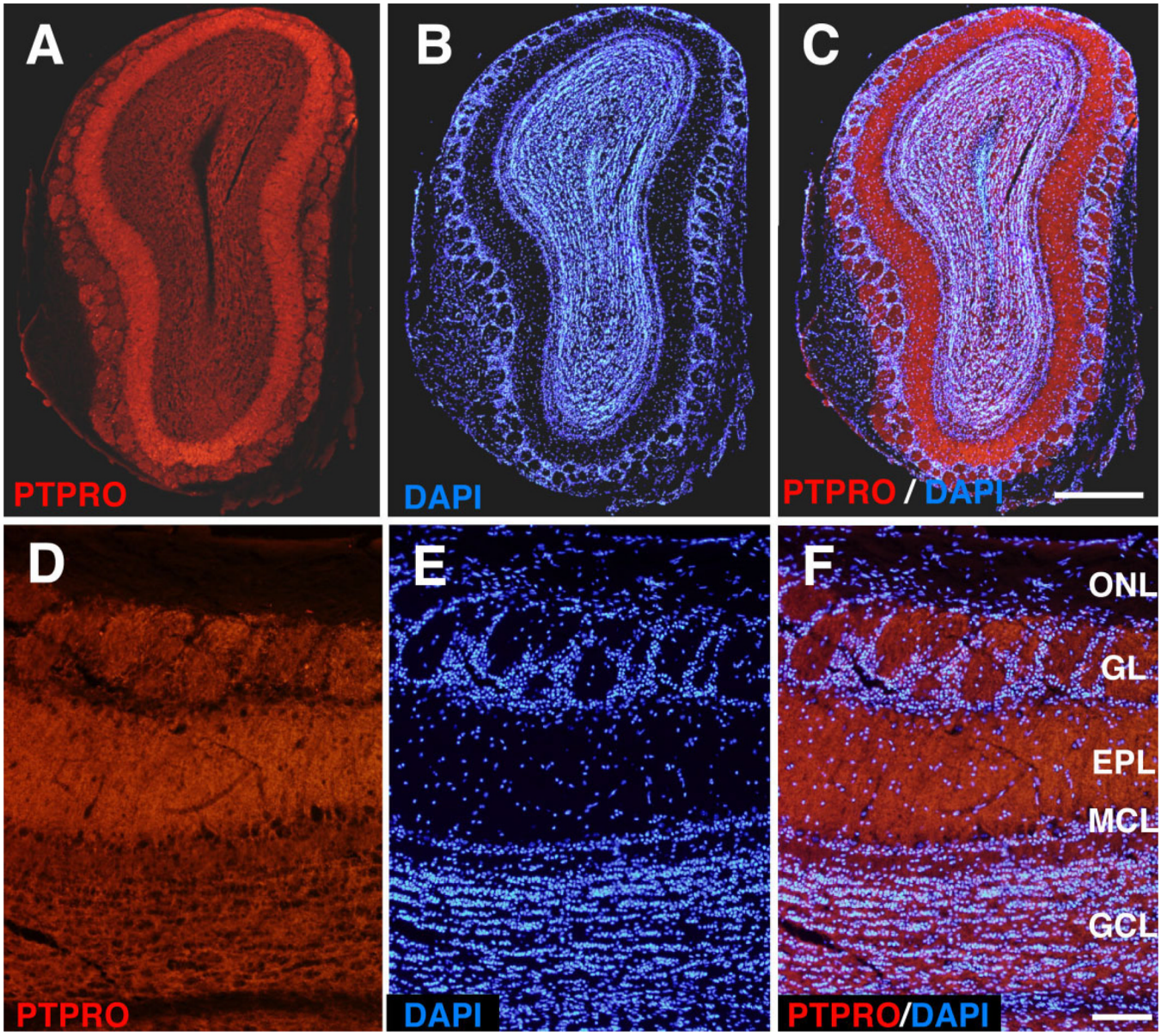

Figure 3.

Distribution of PTPRO immunoreactivity in the adult mouse OB. **A–F:** Coronal cryosection of the adult mouse OB (at P8w) immunostained with the mAb to PTPRO (A,D, red) together with DAPI (B,E, blue). The merged images are shown in C,F. In D–F, the images from A–C are captured at higher magnification to show the localization of PTPRO immunoreactivity in five neural layers of the OB. PTPRO immunostaining is most prominent in the external plexiform layer (EPL). PTPRO immunostaining is also observed in the glomerular layer (GL) and granule cell layer (GCL), whereas it is absent in the mitral cell layer (MCL) and olfactory nerve layer (ONL) as well as at the border area between the GL and the EPL. All images were acquired with a fluorescence microscope (BX51; Olympus). Scale bars = 500 μm in C (applies to A–C); 100 μm in F (applies to D–F).

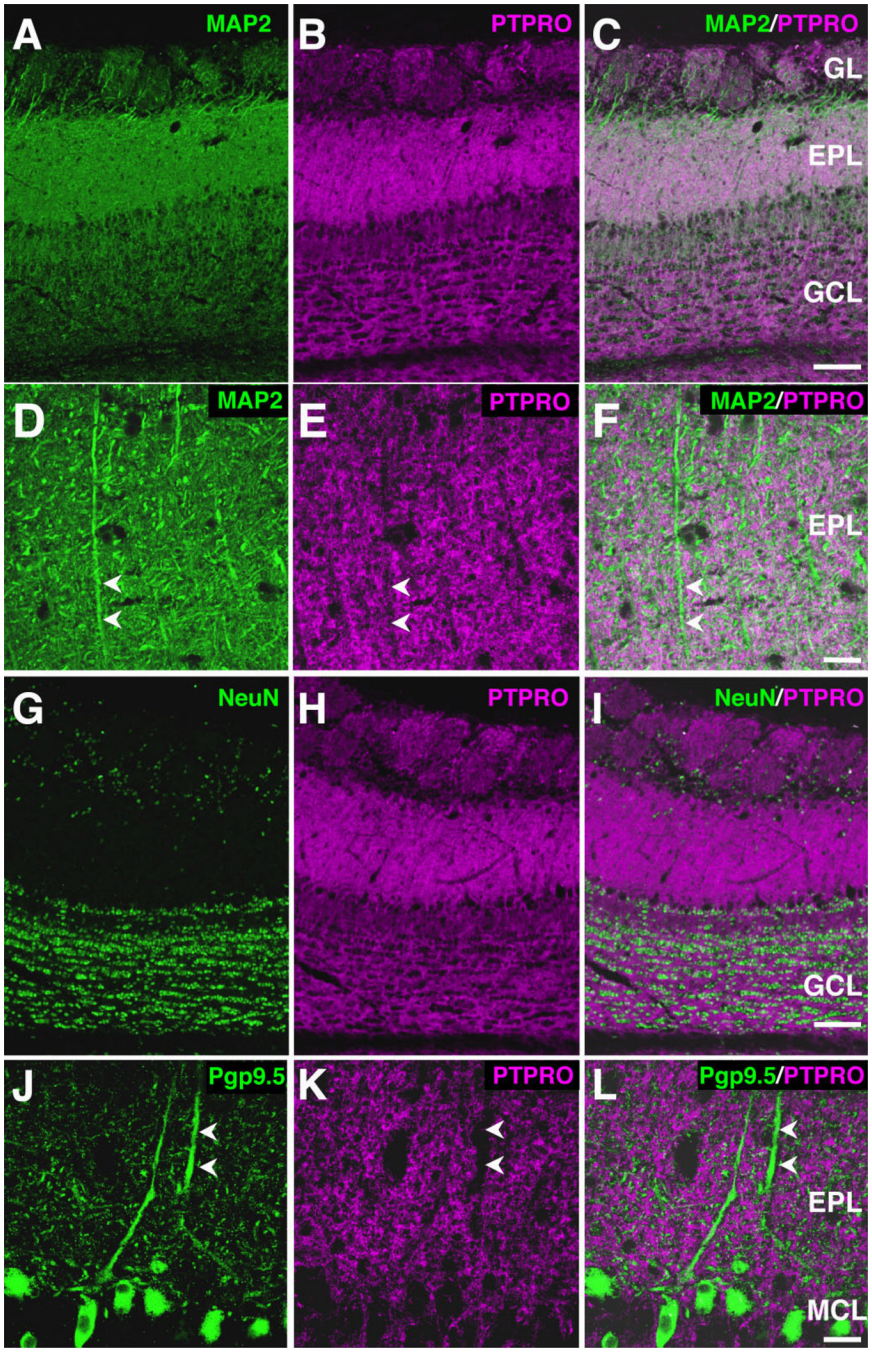

Figure 4.

Expression of PTPRO in the EPL of the adult mouse OB. **A–F:** Coronal cryosection of the adult mouse OB (at P8w) immunostained with mAbs to microtubule-associated protein 2 (MAP2; A,D, green) and PTPRO (B,E, magenta). The merged images are shown in C,F. Confocal images of the EPL at higher magnification are shown in D–F. In A–C, PTPRO staining overlaps extensively with that of MAP2, a dendrite marker, in the EPL and GL as well as the outer layer of the GCL. In D–F, PTPRO staining is observed as a reticular or dot-like structure in the EPL and does not overlap with MAP2 staining on the thick neurites (arrowheads), which are presumed to be mitral/tufted cell dendrites. **G–I:** Coronal cryosection of the adult mouse OB also immunostained with mAbs to neuronal nuclei

(NeuN, a marker for the nucleus of mature neurons; G, green) and PTPRO (H, magenta). The merged image is shown in I. PTPRO staining does not overlap with that of NeuN. **J–L:** Coronal cryosection of the EPL and MCL immunostained with mAbs to protein gene product 9.5 (Pgp9.5, a marker for mitral/tufted cells in the adult OB; J, green) and PTPRO (K, magenta). The merged image is shown in L. PTPRO staining does not overlap with that of Pgp9.5 in the EPL or MCL, suggesting that PTPRO is not expressed in mitral/tufted cells. Arrowheads indicate Pgp9.5-positive neurites likely derived from mitral cells in the MCL. Images for A–C and G–I were acquired with a fluorescence microscope (BX51; Olympus), and those for D–F and J–L were acquired with a laser scanning confocal microscope (LSM5 Pascal; Carl Zeiss). Scale bars = 100 μm in C (applies to A–C); 20 μm in F (applies to D–F); 100 μm in I (applies to G–I); 20 μm in L (applies to J–L).

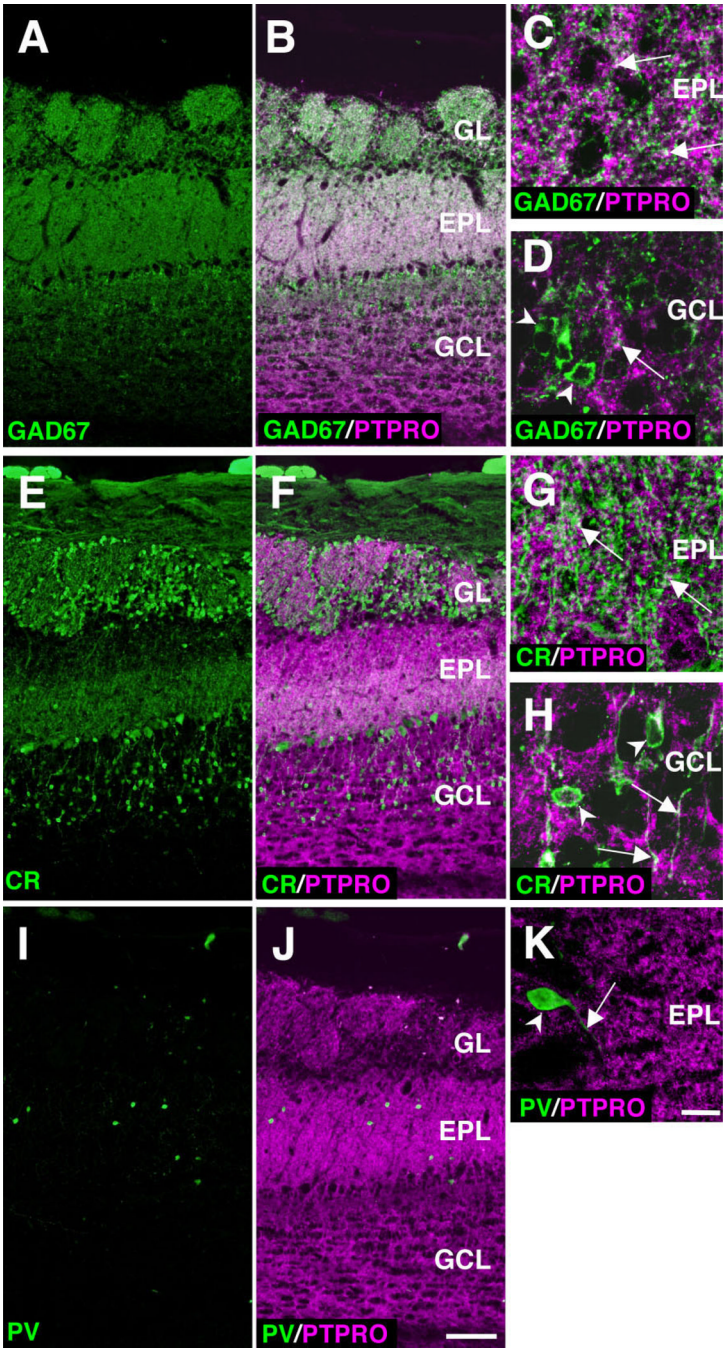

Figure 5.

Localization of PTPRO in the GABAergic or CR-positive granule cells. **A–D:** Coronal cryosection of the adult mouse OB (at P8w) immunostained with mAbs to glutamic acid decarboxylase 67 (GAD67; A,B, green) and PTPRO (B, magenta). The merged image is shown in B. GAD67 staining is predominant in the EPL and GL as well as the outer part of the GCL. GAD67 staining overlaps extensively with that of PTPRO in the EPL. The merged images of the EPL (C) and GCL (D) at higher magnification are also shown. GAD67 and PTPRO staining frequently colocalize in dot-like structures (C, arrows). The somas of GAD67-positive neurons are present in the GCL (D, arrowheads). PTPRO staining is minimal in the somas of GAD67-positive neurons in the GCL but overlaps with GAD67-

positive dot-like structures (D, arrow). **E–H:** Coronal cryosection of the adult mouse OB immunostained with mAbs to calretinin (CR; E,F, green) and PTPRO (F, magenta). The merged image is shown in F. CR staining partially overlaps with that of PTPRO in the GL and EPL as well as GCL. The merged images of the EPL (G) and GCL (H) at higher magnification are also shown. CR and PTPRO staining frequently colocalizes in dot-like structures in EPL (G, arrows). The somas of CR-positive neurons are present in the GCL (H, arrowheads). CR staining in the GCL partially overlaps with that of PTPRO in the somas of the CR-positive neurons (H, arrowheads) as well as in neurite-like structures (H, arrows). **I–K:** Coronal cryosection of the adult mouse OB immunostained with mAbs to parvalbumin (PV; I,J, green) and PTPRO (J, magenta). The merged image is shown in J. The merged image of the EPL at higher magnification is also shown in K. PV staining barely overlaps that of PTPRO in either somas (arrowhead) or neurites (arrow) in the EPL. The images in A,B,E,F,I,J were acquired with a fluorescence microscope (BX51; Olympus). Those for C,D,G,H,K were acquired with a laser scanning confocal microscope (LSM5 Pascal; Carl Zeiss). Scale bars = 100 μm in J (applies to A,B,E,F,I,J); 20 μm in K (applies to C,D,G,H,K).

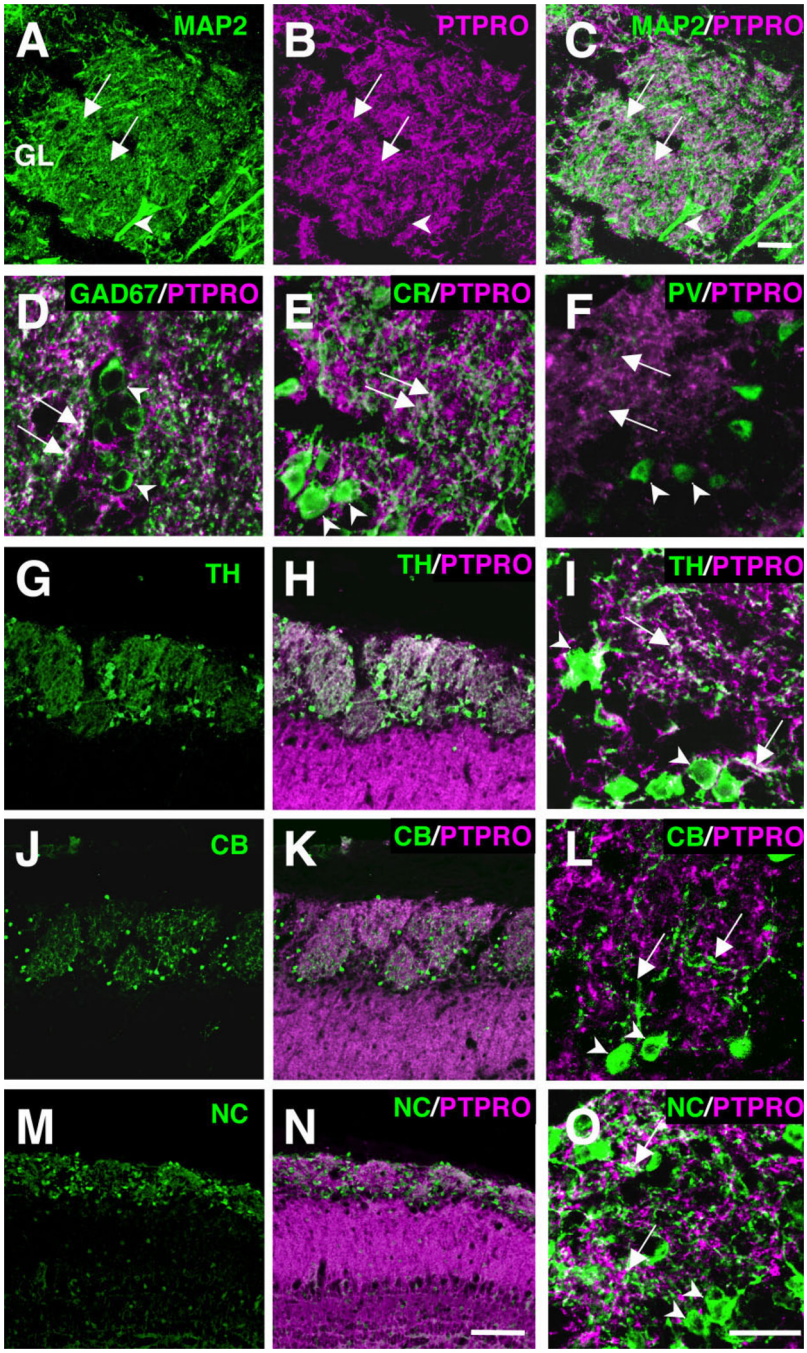

Figure 6.

Localization of PTPRO in periglomerular cells. **A–C:** Coronal cryosection of the adult mouse OB (at P8w) immunostained with mAbs to MAP2 (A, green) and PTPRO (B, magenta). The merged image is shown in C. The meshwork-like staining of PTPRO, which enwrapped each glomerulus, is shown in B. Such staining of PTPRO partially overlaps with that of MAP2 (A) in the GL (A–C, arrows). Howrever, PTPRO staining does not overlap with thick MAP2-positive neurites, which are thought to be dendrites derived from mitral/tufted cells (A–C, arrowheads). **D–F:** Coronal cryosection of the adult mouse OB immunostained with mAbs to GAD67 (D, green), CR (E, green), or PV (F, green) and

PTPRO (D–F, magenta). The merged images are shown in D–F. PTPRO and GAD67 staining colocalizes in dot-like or neurite-like structures in the GL (D, arrows). In contrast, PTPRO staining is minimal in somas of GAD67-positive neurons (D, arrowheads). PTPRO and CR staining colocalizes in neurite-like structures in the GL (E, arrows), but PTPRO staining is minimal in the somas of CR-positive neurons (E, arrowheads). PV staining barely overlaps that of PTPRO in either somas (F, arrowheads) or neurites (F, arrows) in the GCL. **G–I:** Coronal cryosection of the adult mouse OB immunostained with mAbs to tyrosine hydroxylase (TH; G,H, green) and PTPRO (H, magenta). The merged image is shown in H. PTPRO staining partially overlaps with that of TH in the GL. The merged image of the GL at higher magnification is also shown in I. PTPRO and TH staining in the GL colocalizes along neurite-like or dot-like structures (I, arrows). PTPRO staining is also observed in the soma (I, arrowheads). **J–L:** Coronal cryosection of the adult mouse OB immunostained with pAbs to calbindin D28k (CB; J,K, green) and the mAb to PTPRO (K, magenta). The merged image is shown in K. The merged image of the GL at higher magnification is also shown in L. PTPRO staining in the GL does not overlap with that of CB in the either somas (arrowheads) or neurite-like structures (arrows). **M–O:** Coronal cryosection of the adult mouse OB immunostained with pAbs to neurocalcin (NC; M,N, green) and PTPRO (N, magenta). The merged image is shown in N. PTPRO staining partially overlaps with that of NC in the GL. The merged image of the GL at higher magnification is also shown in O. PTPRO and NC staining in the GL colocalizes along neurite-like or dot-like structures (O, arrows). In contrast, PTPRO staining is minimal in somas of NC-positive neurons (O, arrowheads). The images for G,H,J,K,M,N were acquired with a fluorescence microscope (BX51; Olympus). Those for A–F,I,L,O were acquired with a laser scanning confocal microscope (LSM5 Pascal; Carl Zeiss). Scale bars = 20 μm in C (applies to A–C); 100 μm in N (applies to G,H,J,K,M,N); 20 μm in O (applies to D–F,I,L,O).

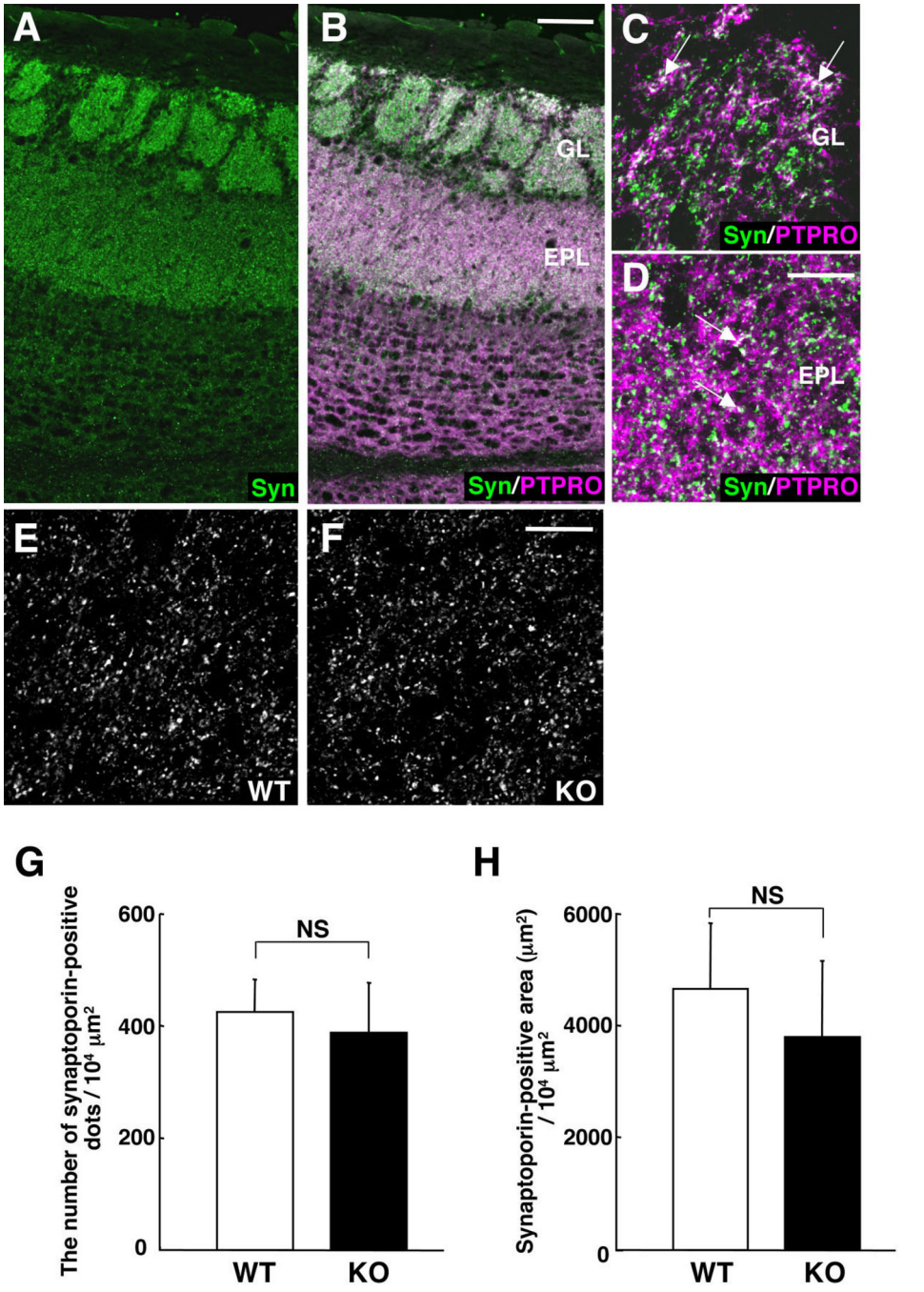

Figure 7.

Costaining of PTPRO and synaptoporin in the GL and the EPL. **A–D:** Coronal cryosection of the adult mouse OB (at P8w) immunostained with pAbs to synaptoporin (A,B, green) and the mAb to PTPRO (B, magenta). The merged image is shown in B. PTPRO staining overlaps extensively with that of synaptoporin in the GL and EPL. The merged images of the GL (C) and EPL (D) are also shown at higher magnification. PTPRO staining frequently overlaps with dot-like staining of synaptoporin (arrows) in the GL and the EPL. **E,F:** Sagittal cryosections of the OB from wild-type (E, WT) or PTPRO-deficient (F, KO) mice at 5 weeks after birth immunostained with pAbs to synaptoporin. The images show the

staining of synaptoporin in the EPL. **G:** The number of immunoreactive dots of synaptoporin per 10^4 μm^2 in the EPL of either wild-type or PTPRO-deficient mice. The number of dots was determined in ImageJ (n = 10 sections). **H:** The synaptoporin-positive area (square micrometers) per 10^4 μm^2 in the EPL of either wild-type or PTPRO-deficient mice was determined in ImageJ (n = 10 sections). Data are means ± SD from 10 sections of each genotype. Statistical analysis was performed by Student's *t*-test. $P > 0.05$ was considered statistically not significant. NS, not significant. The images for A,B were acquired with a fluorescence microscope (BX51; Olympus). Those for C–F were acquired with a laser scanning confocal microscope (LSM5 Pascal; Carl Zeiss). Scale bars = 100 μm in B (applies to A,B); 20 μm in D (applies to C,D); 20 μm in F (applies to E,F).

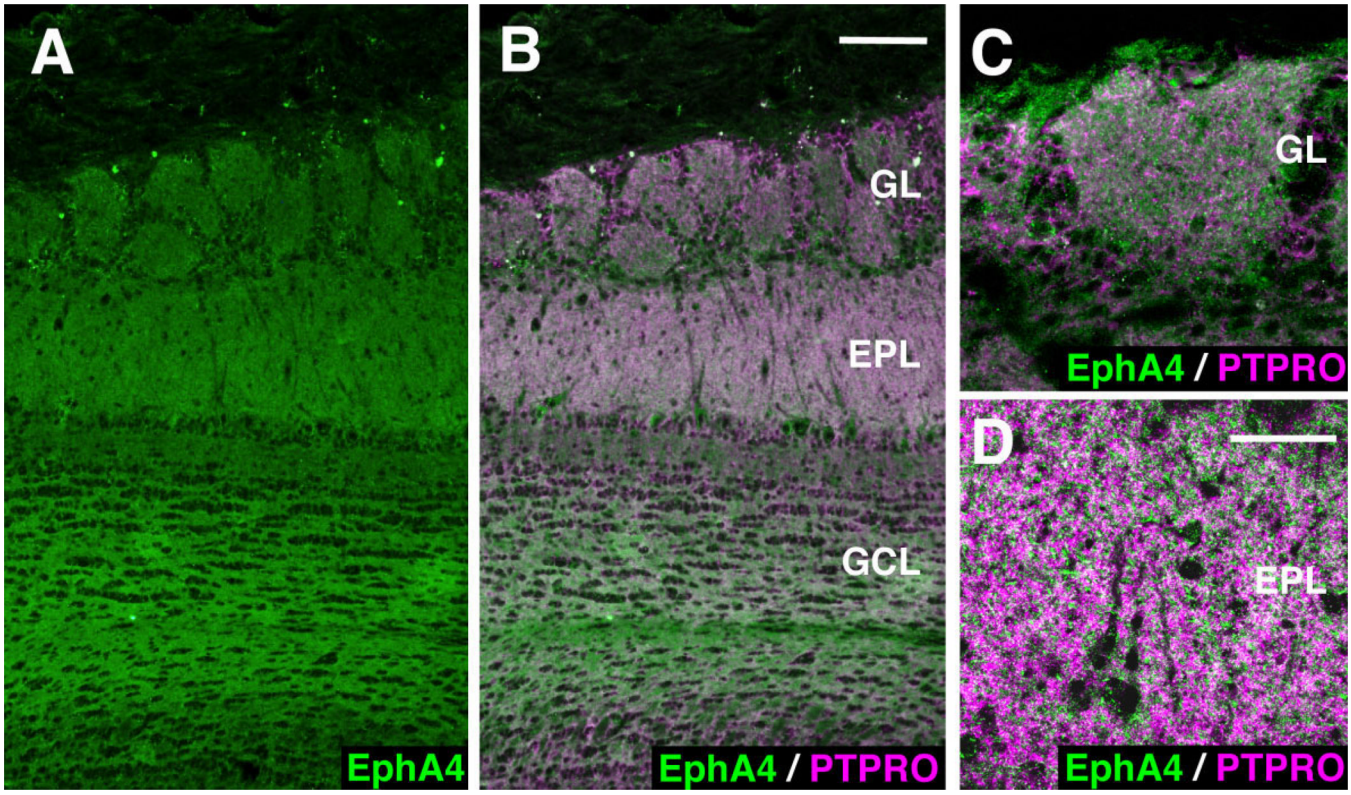

Figure 8.

Costaining of PTPRO and EphA4. **A–D:** Coronal cryosection of the adult mouse OB (at P8w) immunostained with pAbs to EphA4 (A,B, green) and the mAb to PTPRO (B, magenta). The merged image is shown in B. The staining of PTPRO overlaps extensively with that of EphA4 in the GL, EPL, and GCL. The merged images of the GL (C) and EPL (D) are also shown at higher magnification. The images for A,B were acquired with a fluorescence microscope (BX51; Olympus). Those for C and D were acquired with a laser scanning confocal microscope (LSM5 Pascal; Carl Zeiss). Scale bars = 100 μm in B (applies to A,B); 20 μm in D (applies to C,D).

TABLE 1

Primary Antibodies Used in This Study[1]

Antigen	Immunogen	Manufacturer, species, type, catalog No.	Dilution used for IF or IB
Calbindin D28K	Recombinant mouse calbindin	Millipore (Chemicon, Temecula, CA), rabbit polyclonal, AB1778	1:1,000, IF
Calretinin	Recombinant rat calretinin	Millipore (Chemicon), mouse monoclonal, MAB1568	1:1,000, IF
EphA4	GST EphA4 fusion protein corresponding to the SAM domain and C-terminal tail (residues 909-986) of mouse EphA4	Millipore (Upstate, Lake Placid, NY), rabbit polyclonal, 07-309	1:200, IF
GAD67	Recombinant GAD67 protein	Millipore (Chemicon), mouse monoclonal, MAB5406	1:1,000, IF
MAP2	Rat brain microtubule-associated proteins	Sigma (St. Louis, MO), mouse monoclonal, M4403	1:1,000, IF
NeuN	Purified cell nuclei from mouse brain	Millipore (Chemicon), mouse monoclonal, MAB377	1:200, IF
Neurocalcin	Recombinant rat neurocalcin δ	Enzo Life Science (Farmingdale, NY), rabbit polyclonal, NL3770	1:500, IF
Parvalbumin	Purified frog muscle parvalbumin	Sigma, mouse monoclonal, P3088	1:1,000, IF
Pgp9.5	Native protein gene product 9.5 (PGP9.5) from human brain	AbD Serotec (Oxford, United Kingdom), mouse monoclonal, 7863-2004	1:500, IF
PTPRO	Recombinant PTPRO-Fc fusion protein; the extracellular domain of mouse PTPRO (amino acids 1-442) fused with the Fc region of human IgG	This paper	1:200, IF 1:500, IB
Synaptoporin	Synthetic peptide (EFGQQPSGPTSFNN) corresponding to residues 250–263 (rat sequence) coupled to keyhole limpet hemocyanin via an added N-terminal cysteine residue	Synaptic System (Göttingen, Germany), rabbit polyclonal, 102002	1:1,000, IF
Tyrosine hydroxylase	Tyrosine hydroxylase purified from PC12 Cells	Millipore (Chemicon), mouse monoclonal, MAB318	1:500, IF

[1] IF, immunohistofluorescence; IB, immunoblot.